Title	Reconstruction of surfaces of revolution from single uncalibrated views
Author(s)	Wong, KYK; Mendonça, PRS; Cipolla, R
Citation	Image And Vision Computing, 2004, v. 22 n. 10 SPEC. ISS., p. 829-836
Issued Date	2004
URL	http://hdl.handle.net/10722/48430
Rights	Creative Commons: Attribution 3.0 Hong Kong License

Reconstruction of Surfaces of Revolution from Single Uncalibrated Views

Kwan-Yee K. Wong [a,*], Paulo R. S. Mendonça [b], Roberto Cipolla [c]

[a] *Dept. of Comp. Science and Info. Systems, The University of Hong Kong, Pokfulam Road, HK*

[b] *GE Global Research Center, Schenectady, NY 12301, USA*

[c] *Department of Engineering, University of Cambridge, Cambridge, CB2 1PZ, UK*

Abstract

This paper addresses the problem of recovering the 3D shape of a surface of revolution from a single uncalibrated perspective view. The algorithm introduced here makes use of the invariant properties of a surface of revolution and its silhouette to locate the image of the revolution axis, and to calibrate the focal length of the camera. The image is then normalized and rectified such that the resulting silhouette exhibits bilateral symmetry. Such a rectification leads to a simpler differential analysis of the silhouette, and yields a simple equation for depth recovery. It is shown that under a general camera configuration, there will be a 2-parameter family of solutions for the reconstruction. The first parameter corresponds to an unknown scale, whereas the second one corresponds to an unknown attitude of the object. By identifying the image of a latitude circle, the ambiguity due to the unknown attitude can be resolved. Experimental results on real images are presented, which demonstrate the quality of the reconstruction.

Key words: surface of revolution; silhouette; single view geometry; harmonic homology.

1 Introduction

2D images contain cues to surface shape and orientation. However, their interpretation is inherently ambiguous because depth information is lost during the image formation process when 3D structures in the world are projected onto 2D images.

* Corresponding author.
Email addresses: kykwong@csis.hku.hk (Kwan-Yee K. Wong), mendonca@crd.ge.com (Paulo R. S. Mendonça), cipolla@eng.cam.ac.uk (Roberto Cipolla).

Multiple images from different viewpoints can be used to resolve these ambiguities, and this results in techniques like *stereo vision* and *structure from motion*. On the other hand, under certain appropriate assumptions, it is also possible to infer scene structure, like surface orientation and curvature, from a single image. In this paper, a simple technique for recovering the 3D shape of a surface of revolution from a single view is introduced. The symmetry properties exhibited in the image of a surface of revolution are exploited to calibrate the focal length of the camera, and to rectify the image so that the resulting silhouette exhibits bilateral symmetry. Surface normals along the contour generator are then determined from the rectified silhouette, and depth information can then be recovered using a coplanarity constraint between the surface normal and the revolution axis.

This paper is organized as follows. Section 2 briefly reviews existing techniques in the literature for shape from contour using single view. Section 3 gives the theoretical background necessary for the development of the algorithm presented in this paper. A parameterization for surfaces of revolution is presented and the symmetry properties exhibited in the silhouettes are summarized. In particular, the surface normal and the revolution axis are shown to be coplanar. This coplanarity constraint is exploited in Section 4 to derive a simple technique for reconstructing a surface of revolution from its silhouette in a single view. It is shown that under a general camera configuration, there will be a 2-parameter family of solutions for the reconstruction. The first parameter corresponds to an unknown scale in the reconstruction resulting from the unknown distance of the surface from the camera. The second parameter corresponds to the ambiguity in the orientation of the revolution axis on the y-z plane of the camera coordinate system [1] . The algorithm and implementation are described in Section 5 and results of real data experiments are presented in Section 6. Finally conclusions are given in Section 7.

2 Previous Works

The earliest study of silhouettes in single views dates back to 1978, when Barrow and Tenenbaum [1] showed that surface orientation along the silhouette can be computed directly from image data. In [2], Koenderink showed that the sign of the Gaussian curvature is equal to the sign of the curvature of the silhouette, and convexities, concavities and inflections of the silhouette indicate convex, hyperbolic and parabolic surface points respectively. In [3], Cipolla and Blake showed that the curvature of the silhouette has the same sign as the normal curvature along the contour generator under perspective projection. A similar result was derived for orthographic projection by Brady et al. in [4].

[1] Here we assume a right-handed coordinate system, where the optical center is at the origin, the x-axis and the y-axis point right and down, respectively, and the z-axis is the viewing direction.

In all the above studies, the authors only made use of a single monocular image to infer geometric information from the silhouette. In fact, if some strong a priori knowledge of the object is available, such as the class of shapes to which the object belongs, then a single view alone allows shape recovery. The invariant properties of straight homogeneous generalized cylinders (SHGCs) [5,6] and their silhouettes had been studied by various researchers [7–9], and exploited for object recognition and object pose estimation. In [10–12], algorithms for segmentation and 3D recovery of SHGCs under orthographic projection were presented. In [13], Ulupinar and Nevatia addressed the recovery of curved-axis planar right constant generalized cylinders (PRCGCs) under orthographic projection. Their idea was further developed by Zerroug and Nevatia [14] who implemented a technique for segmentation and 3D recovery of both PRCGCs and circular planar right generalized cylinders (circular PRGCs) from a single real image under orthographic projection.

This paper addresses the problem of recovering the 3D shape of a surface of revolution (SOR) from a single view. Surfaces of revolution belong to a subclass of SHGCs, in which the planar cross-section is a circle centered at and orthogonal to its axis. This work is different from the previous ones in that, rather than the orthographic projection model, which is a quite restricted case, the perspective projection model is assumed. In [15], Lavest et al. presented a system for modelling SORs from a set of few monocular images. Their method only works with calibrated cameras, and requires the presence of a perspective image of a latitude circle of the object and some zero-curvature curve points in the silhouette. The algorithm introduced here works with an uncalibrated camera, and it estimates the focal length of the camera directly from the silhouette. Besides, a latitude circle is not necessary as the algorithm will produce a 2-parameter family of SORs under an unknown attitude and scale of the object.

3 Properties of Surfaces of Revolution

Let $\tilde{\mathbf{C}}_{\mathrm{r}}(s) = [X(s)\ Y(s)\ 0]^{\mathrm{T}}$ be a regular and differentiable planar curve on the x-y plane where $X(s) > 0$ for all s. A surface of revolution can be generated by rotating $\tilde{\mathbf{C}}_{\mathrm{r}}$ about the y-axis, and is given by

$$\tilde{\mathbf{S}}_{\mathrm{r}}(s,\theta) = \begin{bmatrix} X(s)\cos\theta \\ Y(s) \\ X(s)\sin\theta \end{bmatrix}, \tag{1}$$

where θ is the angle parameter for a complete circle. The tangent plane basis vectors

$$\frac{\partial \tilde{\mathbf{S}}_{\mathrm{r}}}{\partial s} = \begin{bmatrix} \dot{X}(s)\cos\theta \\ \dot{Y}(s) \\ \dot{X}(s)\sin\theta \end{bmatrix} \quad \text{and} \quad \frac{\partial \tilde{\mathbf{S}}_{\mathrm{r}}}{\partial \theta} = \begin{bmatrix} -X(s)\sin\theta \\ 0 \\ X(s)\cos\theta \end{bmatrix} \tag{2}$$

are independent since $\dot{X}(s)$ and $\dot{Y}(s)$ are never simultaneously zero and $X(s) > 0$ for all s. Hence $\tilde{\mathbf{S}}_{\mathrm{r}}$ is immersed and has a well-defined tangent plane at each point, with the normal given by

$$\mathbf{n}(s,\theta) = \frac{\partial \tilde{\mathbf{S}}_{\mathrm{r}}}{\partial s} \times \frac{\partial \tilde{\mathbf{S}}_{\mathrm{r}}}{\partial \theta} \tag{3}$$

$$= \begin{bmatrix} X(s)\dot{Y}(s)\cos\theta \\ -X(s)\dot{X}(s) \\ X(s)\dot{Y}(s)\sin\theta \end{bmatrix}. \tag{4}$$

Through any point $\tilde{\mathbf{S}}_{\mathrm{r}}(s_0,\theta_0)$ on the surface, there is a *meridian curve* which is the curve obtained by rotating $\tilde{\mathbf{C}}_{\mathrm{r}}$ about the y-axis by an angle $-\theta_0$, and a *latitude circle* which is a circle on the plane $y = Y(s_0)$ and with its center on the y-axis. Note that the meridian curves and the latitude circles are orthogonal to each other, and they form the principal curves of the surface (see fig. 1). It follows from (4) that the surface normal at $\tilde{\mathbf{S}}_{\mathrm{r}}(s_0,\theta_0)$ lies on the plane containing the y-axis and the point $\tilde{\mathbf{S}}_{\mathrm{r}}(s_0,\theta_0)$, and is normal to the meridian curve through $\tilde{\mathbf{S}}_{\mathrm{r}}(s_0,\theta_0)$. By circular symmetry, the surface normals along a latitude circle will all meet at one point on the y-axis.

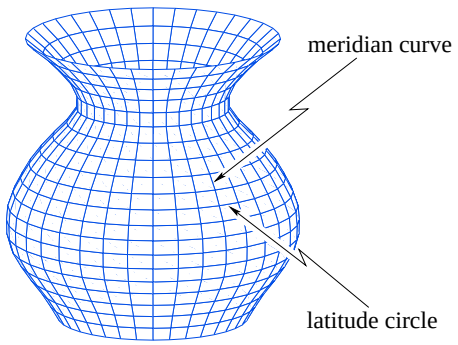

Fig. 1. The meridian curves and latitude circles form the principal curves of the surface of revolution.

Under perspective projection, the image of a surface of revolution will be invariant

to a *harmonic homology* [16,17], given by

$$\mathbf{W} = \mathbb{I}_3 - 2\frac{\mathbf{v}_x \mathbf{l}_\mathrm{s}^\mathrm{T}}{\mathbf{v}_x^\mathrm{T} \mathbf{l}_\mathrm{s}}, \tag{5}$$

where $\mathbf{l}_\mathrm{s}$ is the image of the revolution axis and $\mathbf{v}_x$ is the vanishing point corresponding to the normal direction of the plane that contains the camera center and the revolution axis. Note that $\mathbf{W}$ has four degrees of freedom, and that $\mathbf{v}_x$ and $\mathbf{l}_\mathrm{s}$ are related by [18]

$$\omega \mathbf{v}_x = \mathbf{l}_\mathrm{s}, \tag{6}$$

where $\omega = \mathbf{K}^{-\mathrm{T}}\mathbf{K}^{-1}$ is the image of the absolute conic and $\mathbf{K}$ is the 3×3 calibration matrix of the camera. When the camera is pointing directly towards the revolution axis, $\mathbf{v}_x$ will be at infinity and the harmonic homology will reduce to a *skew symmetry*, given by

$$\mathbf{S} = \frac{1}{\cos(\phi - \theta)} \begin{bmatrix} -\cos(\phi+\theta) & -2\cos\phi\sin\theta & 2d_\mathrm{l}\cos\phi \\ -2\sin\phi\cos\theta & \cos(\phi+\theta) & 2d_\mathrm{l}\sin\phi \\ 0 & 0 & \cos(\phi-\theta) \end{bmatrix}, \tag{7}$$

where $d_\mathrm{l} = u_0\cos\theta + v_0\sin\theta$. The image of the revolution axis and the vanishing point are given by $\mathbf{l}_\mathrm{s} = [\cos\theta \ \sin\theta \ -d_\mathrm{l}]^\mathrm{T}$ and $\mathbf{v}_x = [\cos\phi \ \sin\phi \ 0]^\mathrm{T}$ respectively, and $\mathbf{S}$ has only three degrees of freedom. If the camera also has zero skew and unit aspect ratio, the harmonic homology will then become a *bilateral symmetry*, given by

$$\mathbf{B} = \begin{bmatrix} -\cos 2\theta & -\sin 2\theta & 2d_\mathrm{l}\cos\theta \\ -\sin 2\theta & \cos 2\theta & 2d_\mathrm{l}\sin\theta \\ 0 & 0 & 1 \end{bmatrix}. \tag{8}$$

While $\mathbf{l}_\mathrm{s}$ will have the same form as in the case of skew symmetry, the vanishing point will now be both at infinity and has a direction orthogonal to $\mathbf{l}_\mathrm{s}$. As a result, $\mathbf{B}$ has only two degrees of freedom. These three different cases of symmetry are illustrated in fig. 2.

4 Reconstruction from a Single View

Consider a surface of revolution $\tilde{\mathbf{S}}_\mathrm{r}$ whose revolution axis coincides with the y-axis, and a pin-hole camera $\hat{\mathbf{P}} = [\mathbb{I}_3 \ \mathbf{t}]$ where $\mathbf{t} = [0 \ 0 \ d_z]^\mathrm{T}$ and $d_z > 0$. Let the contour generator be parameterized by s as

$$\tilde{\Gamma}(s) = \tilde{\mathbf{c}} + \lambda(s)\mathbf{p}(s), \text{ where} \tag{9}$$

$$\mathbf{p}(s) \cdot \mathbf{n}(s) = 0. \tag{10}$$

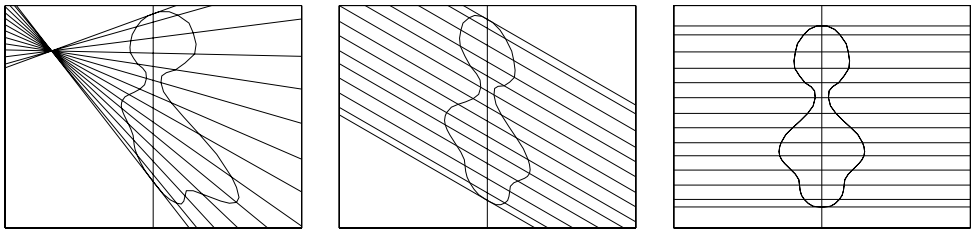

(a) (b) (c)

Fig. 2. (a) Silhouette of a surface of revolution under general perspective projection. The symmetry of the silhouette is described by a harmonic homology defined by the image of the revolution axis and a vanishing point. (b) When the camera is pointing directly towards the revolution axis, the harmonic homology reduces to a skew symmetry, where the vanishing point is at infinity. (c) If the camera also has zero skew and unit aspect ratio, the harmonic homology becomes a bilateral symmetry, in which the vanishing point is at infinity and has a direction orthogonal to the image of the revolution axis.

In (9), $\tilde{\mathbf{c}}$ indicates the camera center at $[0\ 0\ -d_z]^{\mathrm{T}}$, $\mathbf{p}(s)$ is the viewing vector from $\tilde{\mathbf{c}}$ to the focal plane at unit distance for the point $\tilde{\Gamma}(s)$, and $\lambda(s)$ is the depth of the point $\tilde{\Gamma}(s)$ from $\tilde{\mathbf{c}}$ along the z direction. Note that $\mathbf{p}(s)$ has the form $[x(s)\ y(s)\ 1]^{\mathrm{T}}$, where $(x(s), y(s))$ is a point in the bilaterally symmetric silhouette. The tangency constraint is expressed in (10), where $\mathbf{n}(s)$ is the unit surface normal at $\tilde{\Gamma}(s)$ and can be determined up to a sign by [3]

$$\mathbf{n}(s) = \frac{\mathbf{p}(s) \times \frac{d\,\mathbf{p}(s)}{d\,s}}{\left|\mathbf{p}(s) \times \frac{d\,\mathbf{p}(s)}{d\,s}\right|} \tag{11}$$

$$= \frac{1}{\alpha_{\mathrm{n}}(s)} \begin{bmatrix} -\dot{y}(s) \\ \dot{x}(s) \\ x(s)\dot{y}(s) - \dot{x}(s)y(s) \end{bmatrix}, \tag{12}$$

where $\alpha_{\mathrm{n}}(s) = \left|\mathbf{p}(s) \times \frac{d\,\mathbf{p}(s)}{d\,s}\right|$. In Section 3, it has been shown that the surface normal $\mathbf{n}(s)$ will lie on the plane containing the y-axis and the point $\tilde{\Gamma}(s)$. This coplanarity constraint can be expressed as

$$\mathbf{n}(s)^{\mathrm{T}}[\mathbf{n}_y]_{\times}\tilde{\Gamma}(s) = 0, \tag{13}$$

where $\mathbf{n}_y = [0\ 1\ 0]^{\mathrm{T}}$. Let $\mathbf{n}(s) = [n_1(s)\ n_2(s)\ n_3(s)]^{\mathrm{T}}$ and expanding (13) gives

$$\begin{bmatrix} n_1(s) & n_2(s) & n_3(s) \end{bmatrix} \begin{bmatrix} 0 & 0 & 1 \\ 0 & 0 & 0 \\ -1 & 0 & 0 \end{bmatrix} \begin{bmatrix} \lambda(s)x(s) \\ \lambda(s)y(s) \\ \lambda(s) - d_z \end{bmatrix} = 0$$

$$\begin{bmatrix} n_1(s) & n_2(s) & n_3(s) \end{bmatrix} \begin{bmatrix} \lambda(s) - d_z \\ 0 \\ -\lambda(s)x(s) \end{bmatrix} = 0$$

$$n_1(s)(\lambda(s) - d_z) - n_3(s)\lambda(s)x(s) = 0. \tag{14}$$

By rearranging (14), the depth of the point $\tilde{\Gamma}(s)$ is given by

$$\lambda(s) = \frac{d_z n_1(s)}{n_1(s) - n_3(s)x(s)}. \tag{15}$$

Hence, the contour generator can be recovered from the silhouette using (9). In homogeneous coordinates, the contour generator is given by

$$\begin{aligned} \Gamma(s) &= \begin{bmatrix} \tilde{\mathbf{c}} + \lambda(s)\mathbf{p}(s) \\ 1 \end{bmatrix} \\ &= \begin{bmatrix} \tilde{\mathbf{c}} + \frac{d_z n_1(s)}{n_1(s) - n_3(s)x(s)}\mathbf{p}(s) \\ 1 \end{bmatrix} \\ &= \begin{bmatrix} d_z \dot{y}(s)x(s) \\ d_z \dot{y}(s)y(s) \\ d_z \alpha_\Gamma(s) \\ \dot{y}(s) - \alpha_\Gamma(s) \end{bmatrix}, \end{aligned} \tag{16}$$

where $\alpha_\Gamma(s) = (\dot{x}(s)y(s) - x(s)\dot{y}(s))x(s)$. Since the distance d_z cannot be recovered from the image, the reconstruction is determined only up to a *similarity transformation*. The surface of revolution can then be obtained by rotating the contour generator about the y-axis, and is given by

$$\tilde{\mathbf{S}}_{\mathrm{r}}(s, \theta) = \begin{bmatrix} X(s)\cos\theta \\ Y(s) \\ X(s)\sin\theta \end{bmatrix}, \tag{17}$$

where $X(s) = \sqrt{(\lambda(s)x(s))^2 + (\lambda(s) - d_z)^2}$ and $Y(s) = \lambda(s)y(s)$.

Now consider an arbitrary pin-hole camera $\mathbf{P}$ by introducing the intrinsic parameters represented by the camera calibration matrix $\mathbf{K}$ to $\hat{\mathbf{P}}$, and by applying the rotation $\mathbf{R}$ to $\hat{\mathbf{P}}$ about its optical center. Hence $\mathbf{P} = \mathbf{K}\mathbf{R}[\mathbb{I}_3\ \mathbf{t}]$ or $\mathbf{P} = \mathbf{H}\hat{\mathbf{P}}$, where $\mathbf{H} = \mathbf{K}\mathbf{R}$. From the discussions presented in Section 3, the resulting silhouette of $\tilde{\mathbf{S}}_{\mathrm{r}}$ will be invariant to a harmonic homology $\mathbf{W}$. Given $\mathbf{K}$ and $\mathbf{W}$, it is possible to rectify the image by a planar homography $\mathbf{H}_{\mathrm{r}}$ so that the silhouette becomes bilaterally symmetric about the line $\hat{\mathbf{l}}_{\mathrm{s}} = [1\ 0\ 0]^{\mathrm{T}}$ (i.e. the y-axis). This corresponds to normalizing the camera by $\mathbf{K}^{-1}$ and rotating the normalized camera until the revolution axis of $\tilde{\mathbf{S}}_{\mathrm{r}}$ lies on the y-z plane of the camera coordinate system. Note that $\mathbf{H}_{\mathrm{r}}$ is not unique, as any homography $\mathbf{H}'_{\mathrm{r}}$, given by $\mathbf{H}'_{\mathrm{r}} = \mathbf{R}_x(\psi)\mathbf{H}_{\mathrm{r}}$ where $\mathbf{R}_x(\psi)$ is a rotation about the x-axis by an angle ψ, will yield a silhouette which will be bilaterally symmetric about $\hat{\mathbf{l}}_{\mathrm{s}}$. There exists a ψ_0 such that $\mathbf{R}_x(\psi_0)\mathbf{H}_{\mathrm{r}}\mathbf{P} = \hat{\mathbf{P}}$ and the surface of revolution can be reconstructed from the rectified image using the algorithm presented above. In general, ψ_0 cannot be recovered from a single image and hence there will be a 2-parameter family of solutions for the contour generator, given by

$$\Gamma^{\psi}(s) = \begin{bmatrix} d_z\dot{y}(s)x(s) \\ d_z\dot{y}(s)(y(s)\cos\psi - \sin\psi) \\ d_z\alpha_{\Gamma}^{\psi}(s) \\ \dot{y}(s)(y(s)\sin\psi + \cos\psi) - \alpha_{\Gamma}^{\psi}(s) \end{bmatrix} \tag{18}$$

where $\alpha_{\Gamma}^{\psi}(s) = \{(\dot{x}(s)y(s) - x(s)\dot{y}(s))\cos\psi - \dot{x}(s)\sin\psi\}x(s)$. The 2-parameter family of surfaces of revolution $\tilde{\mathbf{S}}_{\mathrm{r}}^{\psi}$ can be obtained by rotating Γ^{ψ} about the y-axis. Note that the ambiguities in the reconstruction correspond to (1) the unknown distance of the surface from the camera and (2) the ambiguity of the orientation of the revolution axis on the y-z plane of the camera coordinate system. It can be shown that such ambiguities in the reconstruction cannot be described by a projective transformation (see [19] for the proof). If the image of a latitude circle in the surface of revolution can be located, the orientation of the revolution axis relative to the y-axis of the camera coordinate system can be estimated [20], which removes one degree of freedom in the ambiguities of the reconstruction. Further, if the radius of such a latitude circle is also known, then all the ambiguities in the reconstruction can be resolved.

It is worth mentioning that sometimes due to self-occlusions, it might not be always possible to recover the whole surface of revolution from its silhouette. This situation is illustrated in fig. 3, where part of the neck and the bottom of the vase cannot be reconstructed. Nonetheless, if more images of the surface of revolution are available, it is possible to recover the whole meridian curve, and hence the whole surface of revolution, by combining fragments of the meridian curve obtained from different images.

(a)

(b)

Fig. 3. Due to self-occlusions, it might not be always possible to recover the whole surface of revolution from its silhouette. (a) It is possible to recover the whole surface from the side view of a vase. (b) Part of the neck and the bottom of the vase cannot be reconstructed from this top view due to self-occlusions.

5 Algorithm and Implementation

5.1 Estimation of the Harmonic Homology

The silhouette ρ of a surface of revolution is first extracted from the image by applying a Canny edge detector [21], and the harmonic homology $\mathbf{W}$ that maps each side of ρ to its symmetric counterpart is then estimated by minimizing the geometric distances between the original silhouette ρ and its transformed version $\rho' = \mathbf{W}\rho$ (see fig. 4). This can be done by sampling N evenly spaced points $\mathbf{x}_i$ along ρ and optimizing the cost function

$$\mathrm{Cost}(\mathbf{v}_x, \mathbf{l}_\mathrm{s}) = \sum_{i=1}^{N} \mathrm{dist}(\mathbf{W}(\mathbf{v}_x, \mathbf{l}_\mathrm{s})\mathbf{x}_i, \rho)^2, \tag{19}$$

where $\mathrm{dist}(\mathbf{W}(\mathbf{v}_x, \mathbf{l}_\mathrm{s})\mathbf{x}_i, \rho)$ is the orthogonal distance from the transformed sample point $\mathbf{x}'_i = \mathbf{W}(\mathbf{v}_x, \mathbf{l}_\mathrm{s})\mathbf{x}_i$ to the original silhouette ρ. A very good initialization of $\mathbf{l}_\mathrm{s}$ and $\mathbf{v}_x$ can be obtained using the bitangents of the silhouette (see [18] for details).

5.2 Image Rectification

After the estimation of the harmonic homology $\mathbf{W}$, the image can be rectified so that the silhouette becomes bilaterally symmetric about the line $\mathbf{l} = [1\ 0\ 0]^\mathrm{T}$. Such a rectified image resembles an image that would have been observed by a normalized camera when the axis of the surface of revolution lies on the y-z plane of the camera coordinate system.

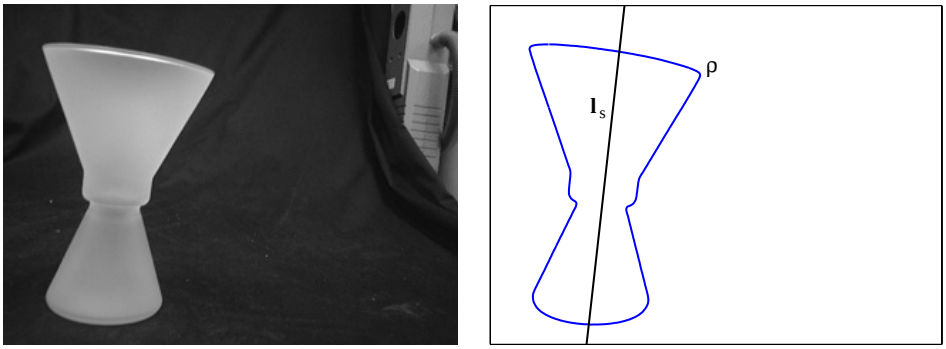

Fig. 4. The silhouette ρ of a surface of revolution (candle holder) is extracted by applying a Canny edge detector and the axis $\mathbf{l}_\mathrm{s}$ of the harmonic homology associated with the silhouette is estimated.

By assuming that the principal point is located at the image center and that the camera has unit aspect ratio, the focal length can be computed from $\mathbf{v}_x$ and $\mathbf{l}_\mathrm{s}$ using (6). The image can then be normalized by $\mathbf{K}^{-1}$ to remove the effects of the intrinsic parameters of the camera. The axis $\mathbf{l}_\mathrm{s}$ of $\mathbf{W}$, and hence the image of the revolution axis, is transformed to $\mathbf{l}_\mathrm{s}^\mathrm{n} = \mathbf{K}^\mathrm{T}\mathbf{l}_\mathrm{s}$.

The normalized image is then transformed by a rotation matrix $\mathbf{R}_\mathrm{b}$ that brings $\mathbf{x}_0^\mathrm{p}$, the orthogonal projection of the principal point $\mathbf{x}_0 = [0\ 0\ 1]^\mathrm{T}$ on the axis $\mathbf{l}_\mathrm{s}^\mathrm{n}$, to $\mathbf{x}_0$. This corresponds to rotating the normalized camera until it points directly towards the axis of the surface of revolution, and the resulting silhouette will then be bilaterally symmetric about the image of the revolution axis. The axis $\mathbf{n}_\mathrm{b}$ and the angle ϕ_b of the rotation $\mathbf{R}_\mathrm{b}$ are given by

$$\mathbf{n}_\mathrm{b} = \frac{\mathbf{x}_0^\mathrm{p} \times \mathbf{x}_0}{|\mathbf{x}_0^\mathrm{p} \times \mathbf{x}_0|}, \text{ and} \tag{20}$$

$$\phi_\mathrm{b} = \arccos\left(\frac{\mathbf{x}_0^\mathrm{p} \cdot \mathbf{x}_0}{|\mathbf{x}_0^\mathrm{p}|\,|\mathbf{x}_0|}\right), \text{ respectively.} \tag{21}$$

After transforming the normalized image by the homography $\mathbf{R}_\mathrm{b}$, the resulting silhouette $\rho^\mathrm{b} = \mathbf{R}_\mathrm{b}\mathbf{K}^{-1}\rho$ will be bilaterally symmetric about the transformed image of the revolution axis, given by $\mathbf{l}_\mathrm{s}^\mathrm{b} = \mathbf{R}_\mathrm{b}\mathbf{l}_\mathrm{s}^\mathrm{n} = [\cos\theta^\mathrm{b}\ \ \sin\theta^\mathrm{b}\ 0]^\mathrm{T}$.

The resulting image is then rotated about the point $\mathbf{x}_0$ until the axis of symmetry aligns with the y-axis, and the transformation is given by $\mathbf{R}_\mathrm{a}$ which is a rotation about the z-axis by an angle $-\theta^\mathrm{b}$. This corresponds to rotating the normalized camera, which is now pointing directly towards the axis of the surface of revolution, about its z-axis until the axis of the surface of revolution lies on its y-z plane. The resulting silhouette $\rho^\mathrm{a} = \mathbf{R}_\mathrm{a}\rho^\mathrm{b}$ is now bilaterally symmetric about the line $\mathbf{l}_\mathrm{s}^\mathrm{a} = \mathbf{R}_\mathrm{a}\mathbf{l}_\mathrm{s}^\mathrm{b} = [1\ 0\ 0]^\mathrm{T}$. The overall transformation for the rectification is given by $\mathbf{H}_\mathrm{r} = \mathbf{R}_\mathrm{a}\mathbf{R}_\mathrm{b}\mathbf{K}^{-1}$, and the rectification process is illustrated in fig. 5.

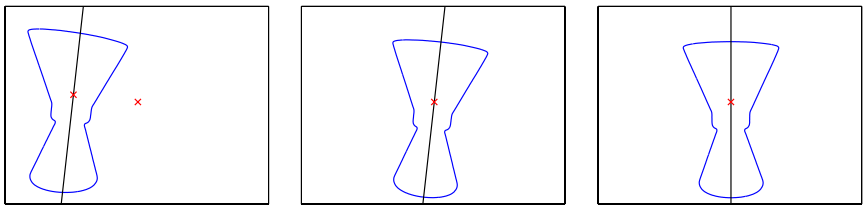

(a) (b) (c)

Fig. 5. (a) The harmonic homology associated with the silhouette of the surface of revolution is estimated, which yields the image of the revolution axis. The image is then normalized by $\mathbf{K}^{-1}$, and the orthogonal projection $\mathbf{x}_0^{\mathrm{p}}$ of the point $\mathbf{x}_0 = [0\ 0\ 1]^{\mathrm{T}}$ on the image of the revolution axis is located. (b) The image is transformed by the homography $\mathbf{R}_b$ so that the point $\mathbf{x}_0$ lies on the image of the revolution axis and the silhouette becomes bilaterally symmetric about the image of the revolution axis. (c) Finally, the image is rotated about the point $\mathbf{x}_0$ until the image of the revolution axis aligns with the y-axis.

5.3 Depth Recovery

Since the rectified silhouette ρ^{a} is bilaterally symmetric about the y-axis, only one side of ρ^{a} needs to be considered during the reconstruction of the surface of revolution. The apparent contour is first segmented manually from the rectified silhouette. This can usually be done easily by removing the topmost and bottommost elliptical parts of the silhouette, which are the images of the topmost and bottommost latitude circles, respectively. Points are then sampled from the apparent contour and the tangent vector (i.e. $\dot{x}(s)$ and $\dot{y}(s)$) at each sample point is estimated by fitting a polynomial to the neighboring points. Points that do not have well-defined tangents are discarded. The surface normal associated with each sample point is then computed using (12). Finally, the depth of each sample point is recovered using (15), and the contour generator and the surface of revolution follow. For $\psi \neq 0$, the viewing vector $\mathbf{p}(s)$ and the associated surface normal $\mathbf{n}(s)$ at each sample point are first transformed by $\mathbf{R}_x(\psi)$. The transformed viewing vector is then normalized so that its 3^{rd} coefficient becomes 1, and (15) can then be used to recover the depth of the sample point.

6 Experiments and Results

Fig. 6 shows the reconstruction of a candle holder. The rectification of the silhouette (see fig. 6(b)) was done using the algorithm described in Section 5. An ellipse was fitted to the bottom of the rectified silhouette for computing the orientation of the revolution axis. The radius of the topmost circle and the height of the candle holder, measured manually using a ruler with a resolution of 1 mm, were 5.7 cm and 17.1 cm respectively. The ratio of the radius of the topmost circle to the height of the reconstructed candle holder (see fig. 6(c)) was 0.3360. This ratio agreed with

the ground truth value (5.7/17.1 = 0.3333) and had a relative error of 0.81% only. Another example is given in fig. 7, which shows the reconstruction of a bowl. The radius of the topmost circle and the height of the bowl were 6.4 cm and 6.2 cm respectively. The ratio of the radius of the topmost circle to the height of the reconstructed bowl (see fig. 7(c)) was 1.0474. This ratio was close to the ground truth value (6.4/6.2 = 1.0323) and had a relative error of 1.46%.

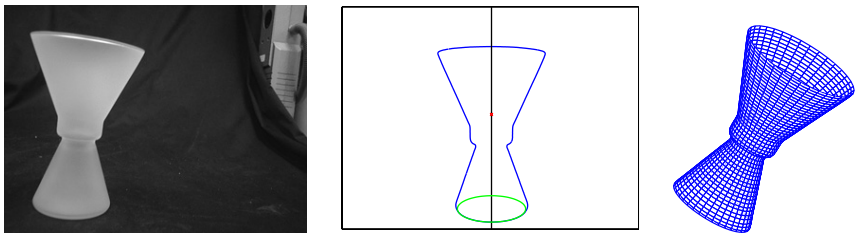

(a) (b) (c)

Fig. 6. (a) Image of a candle holder. (b) Rectified silhouette of the candle holder which exhibits bilateral symmetry. (c) Reconstructed model of the candle holder.

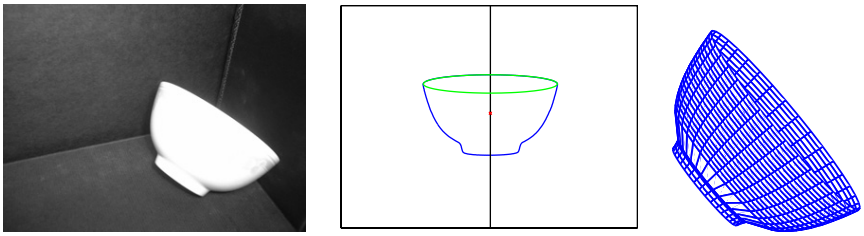

(a) (b) (c)

Fig. 7. (a) Image of a bowl. (b) Rectified silhouette of the bowl which exhibits bilateral symmetry. (c) Reconstructed model of the bowl.

7 Conclusions

By exploiting the coplanarity constraint between the revolution axis and the surface normal, a simple technique for recovering the 3D shape of a surface of revolution from a single view has been developed. The technique presented here assumes perspective projection and uses information from the silhouette only. The invariant properties of the surface of revolution and its silhouette have been used to calibrate the focal length of the camera, and to rectify the image so that the silhouette becomes bilaterally symmetric about the y-axis. This simplifies the analysis of the general camera configuration case to one in which the revolution axis lies on the y-z plane of the camera coordinate system. If the image of a latitude circle in the surface of revolution can be located, the orientation of the revolution axis relative to the y-axis of the camera coordinate system can be estimated, which removes one degree of freedom in the ambiguities of the reconstruction. The remaining degree

of freedom (i.e. scale) can be resolved by knowing the radius of the located latitude circle.

Acknowledgements

The work described in this paper was partially supported by a research grant from The University of Hong Kong.

References

[1] H. G. Barrow, J. M. Tenenbaum, Recovering intrinsic scene characteristics from images, in: A. R. Hanson, E. M. Riseman (Eds.), Computer Vision Systems, Academic Press, New York, 1978, pp. 3–26.

[2] J. J. Koenderink, What does the occluding contour tell us about solid shape?, Perception 13 (1984) 321–330.

[3] R. Cipolla, A. Blake, Surface shape from the deformation of apparent contours, Int. Journal of Computer Vision 9 (2) (1992) 83–112.

[4] M. Brady, J. Ponce, A. L. Yuille, H. Asada, Describing surfaces, Computer Vision, Graphics and Image Processing 32 (1) (1985) 1–28.

[5] T. O. Binford, Visual perception by computer, in: Proc. IEEE Conf. Systems and Control, Miami, FL, 1971, (unpublished).

[6] T. O. Binford, Generalized cylinder representation, in: S. C. Shapiro (Ed.), Encyclopedia of Artificial Intelligence, John Wiley & Sons, 1987, pp. 321–323.

[7] R. Horaud, M. Brady, On the geometric interpretation of image contours, Artificial Intelligence 37 (1988) 333–353.

[8] J. Ponce, D. M. Chelberg, W. B. Mann, Invariant properties of straight homogeneous generalized cylinders and their contours, IEEE Trans. on Pattern Analysis and Machine Intelligence 11 (9) (1989) 951–966.

[9] J. Liu, J. L. Mundy, D. A. Forsyth, A. Zisserman, C. A. Rothwell, Efficient recognition of rotationally symmetric surface and straight homogeneous generalized cylinders, in: Proc. Conf. Computer Vision and Pattern Recognition, New York, NY, 1993, pp. 123–129.

[10] H. Sato, T. O. Binford, Finding and recovering SHGC objects in an edge image, Computer Vision, Graphics and Image Processing 57 (3) (1993) 346–358.

[11] A. D. Gross, T. E. Boult, Recovery of SHGCs from a single intensity view, IEEE Trans. on Pattern Analysis and Machine Intelligence 18 (2) (1996) 161–180.

[12] M. Zerroug, R. Nevatia, Volumetric descriptions from a single intensity image, Int. Journal of Computer Vision 20 (1/2) (1996) 11–42.

[13] F. Ulupinar, R. Nevatia, Shape from contour: Straight homogeneous generalized cylinders and constant cross-section generalized cylinders, IEEE Trans. on Pattern Analysis and Machine Intelligence 17 (2) (1995) 120–135.

[14] M. Zerroug, R. Nevatia, Three-dimensional descriptions based on the analysis of the invariant and quasi-invariant properties of some curved-axis generalized cylinders, IEEE Trans. on Pattern Analysis and Machine Intelligence 18 (3) (1996) 237–253.

[15] J. M. Lavest, R. Glachet, M. Dhome, J. T. La Preste, Modelling solids of revolution by monocular vision, in: Proc. Conf. Computer Vision and Pattern Recognition, Lahaina, Maui, HI, 1991, pp. 690–691.

[16] A. Zisserman, J. L. Mundy, D. A. Forsyth, J. Liu, N. Pillow, C. Rothwell, S. Utcke, Class-based grouping in perspective images, in: Proc. 5th Int. Conf. on Computer Vision, Cambridge, MA, USA, 1995, pp. 183–188.

[17] P. R. S. Mendonça, K.-Y. K. Wong, R. Cipolla, Epipolar geometry from profiles under circular motion, IEEE Trans. on Pattern Analysis and Machine Intelligence 23 (6) (2001) 604–616.

[18] K.-Y. K. Wong, P. R. S. Mendonça, R. Cipolla, Camera calibration from surfaces of revolution, IEEE Trans. on Pattern Analysis and Machine Intelligence 25 (2) (2003) 147–161.

[19] K.-Y. K. Wong, Structure and motion from silhouettes, Ph.D. thesis, Department of Engineering, University of Cambridge (2001).

[20] M. Dhome, J. T. La Preste, G. Rives, M. Richetin, Spatial localization of modelled objects of revolution in monocular perspective vision, in: O. Faugeras (Ed.), Proc. 1st European Conf. on Computer Vision, Vol. 427 of Lecture Notes in Computer Science, Springer–Verlag, Antibes, France, 1990, pp. 475–485.

[21] J. Canny, A computational approach to edge detection, IEEE Trans. on Pattern Analysis and Machine Intelligence 8 (6) (1986) 679–698.